JOURNAL OF MATERIALS SCIENCE 26 (1991) 3969–3976

Early and late mechanical alloying stages of the Pd–Si system

M. MAGINI, N. BURGIO, S. MARTELLI, F. PADELLA, E. PARADISO
Amorphous Material Project, Chemistry and Materials Department, ENEA, C.R.E. Casaccia, Via Anguillarese, Rome, Italy
G. ENNAS
Dipartimento di Scienze Chimiche, Via Ospedale 72, Universita' di Cagliari, Cagliari, Italy

Four Pd–Si compositions (Pd/Si = 2.5/1; 3/1; 4/1 and 5/1) were mechanically alloyed by a ball-milling technique. X-ray diffraction and fluorescence analysis were used to monitor the mechanical alloying (MA) process which was carried out in planetary and vibratory ball mills. The first step of the milling process consists in a very fine fragmentation of the silicon particles into the palladium matrix. After this early stage of milling, formation of the intermetallic line compound Pd_3Si can occur for the 2.5/1, 3/1 and 4/1 composition depending on the milling conditions and/or milling apparatus adopted: i.e. on the conditions of energy transfer experimentally realized. Subsequent milling indicates that amorphization probably occurs starting from the previously formed Pd_3Si compound. Long milling times, up to 56 h, promote a demixing process towards the parent elements for the 2.5/1 and 4/1 compositions. Thermal treatments of the long-term milled samples confirm the final products obtained from the near room-temperature solid state reaction induced by MA. For the Pd_5Si composition the conditions for Pd_3Si formation and subsequent amorphization were never reached.

1. Introduction

Mechanical alloying (MA) is an industrial process known from the early seventies [1]. It was conceived to add a dispersoid phase intimately to an already existent powder alloy in order to improve the properties of the final product. Recently, MA has been exploited to obtain alloys directly without any melting process. Very often the alloys obtained are amorphous or metastable and their compositions are not limited to the deep eutectic regions, as in rapid quenching techniques.

From this new perspective a good deal of work has been done in recent years. Amorphous alloys have been obtained either starting from pure elemental powders (e.g. [2–6]) or from intermetallic compounds (e.g. [6–8]). It has also been noticed that an intermetallic compound can be the first result of the milling of the pure elements [9–12] and that further prolonged milling can subsequently amorphize the intermetallic phase formed [10, 12].

In a previous paper [12] we have reported that the Pd_3Si intermetallic compound is first formed when milling the $Pd_{80}Si_{20}$ and $Pd_{75}Si_{25}$ mixtures of elemental powders. Later, the early milling stages of different Pd–Si compositions, existing around the stoichiometry of Pd_3Si, were examined [13]. In the present work, the various steps of the MA process under different milling conditions were analysed, by investigating the compositions examined previously [13], extending the milling times to 56 h and employing different ball mills.

2. Experimental procedure

2.1. Ball milling

Elemental Pd (60 mesh, 11.97 $g\,cm^{-3}$) and Si powders (70–250 mesh, 2.33 $g\,cm^{-3}$) were mixed to obtained four different compositions: Pd_5Si, Pd_4Si, Pd_3Si, $Pd_{2.5}Si$, of which only the 3/1 ratio corresponds to the stoichiometry of an intermetallic compound.

The MA process was carried out using either a planetary (Fritsch "Pulverisette 5") or a vibratory (SPEX 8000) ball mill. The balls to powder weight ratio was always kept constant to about ten. Tempered steel or tungsten carbide vials were employed with balls of the same material. To avoid oxidation, the vials were sealed under pure argon.

The four compositions under examination were simultaneously milled in the planetary mill, in order to process the samples in exactly the same way. The SPEX 8000 was used, for comparative purposes, to mill the Pd_4Si composition. From time to time the vials were opened and some powder removed. A few milligrams of the powder were used to coat a wide adhesive tape surface to perform both X-ray and fluorescence measurements on the same sample.

2.2. X-ray data

X-ray diffraction patterns of the samples were recorded using an automatic Seifert Pad IV diffractometer, with MoK_α radiation ($\lambda = 0.071\,07$ nm).

2.3. Fluorescence data

The fluorescence analysis was performed using a Link

0022–2461/91 $03.00 + .12

XR-500 X-ray fluorescence system equipped with a silver anode tube. The net interference values were evaluated by selecting the SiK_α and PdL_α peaks.

2.4. Chemical analysis

Quantitative chemical analysis was performed in order to check the silicon content on the final samples after the milling process. The samples were dissolved by alkaline fusion treatment and then analysed by ionic chromatography (Dionex 2020i). The results clearly indicate that no appreciable variation in the silicon content occurred during the milling process. Oxygen analysis was also performed in some of the milled samples by standard LECO apparatus procedures (LECO model EF10 connected with LECO model RO17).

2.5. Thermal treatments

Thermal treatments of the samples milled for 56 h were performed in a furnace under a flux of argon gas at two different temperatures (650 and 850 °C) for 5, 10 and 15 h.

3. Results

3.1. X-ray data

The X-ray patterns, for the four compositions examined, are shown in Figs 1–5 up to a maximum of 56 h milling. The patterns at $t = 0$ and 1 h are reported only for the composition 4/1 (Fig. 1) because they are representative of all the cases examined.

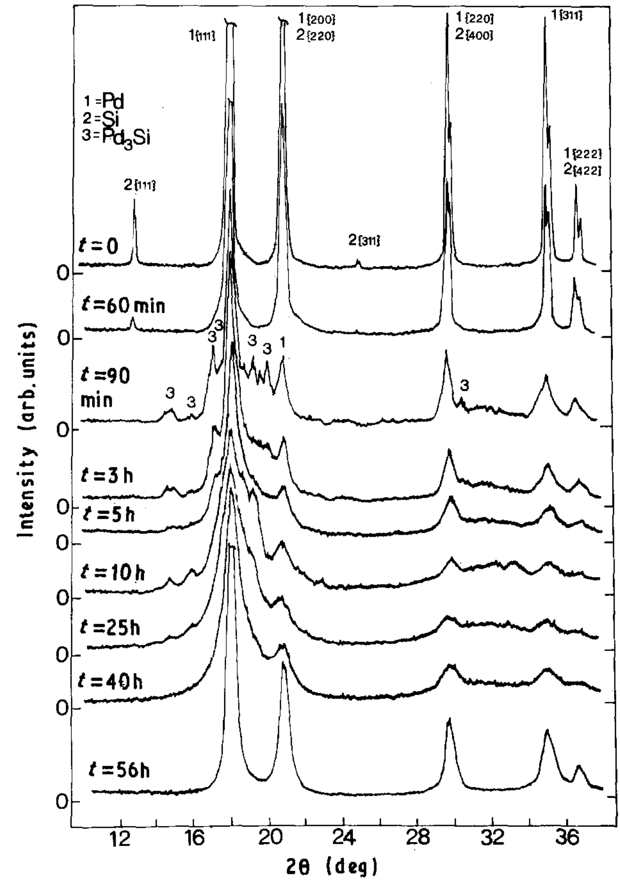

Figure 1 X-ray diffraction patterns of the Pd_4Si (F) composition at various milling times. Patterns at $t = 0$ and 60 min are also representative for the other compositions examined (Figs 2–5). F or S in all figures indicate Fritsch or Spex ball mill.

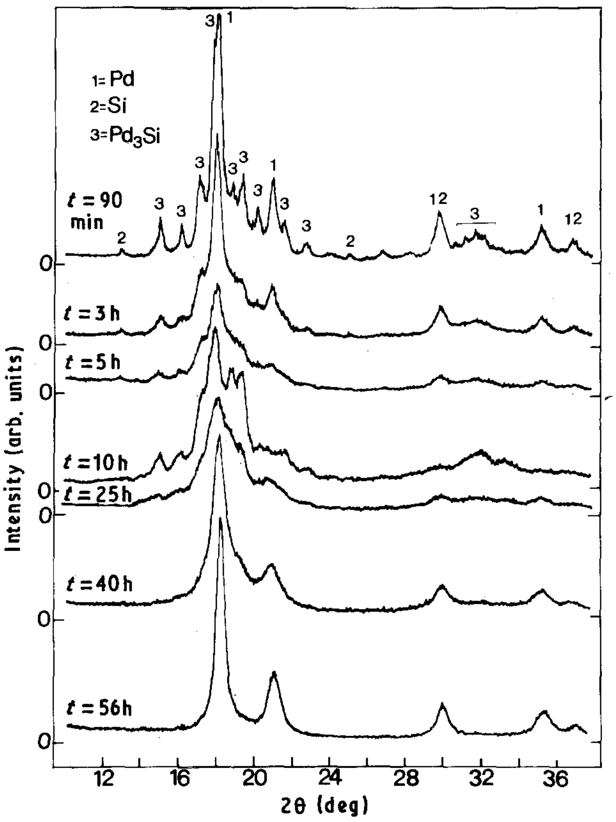

Figure 2 X-ray diffraction patterns of the $Pd_{2.5}Si$ (F) composition at various milling times.

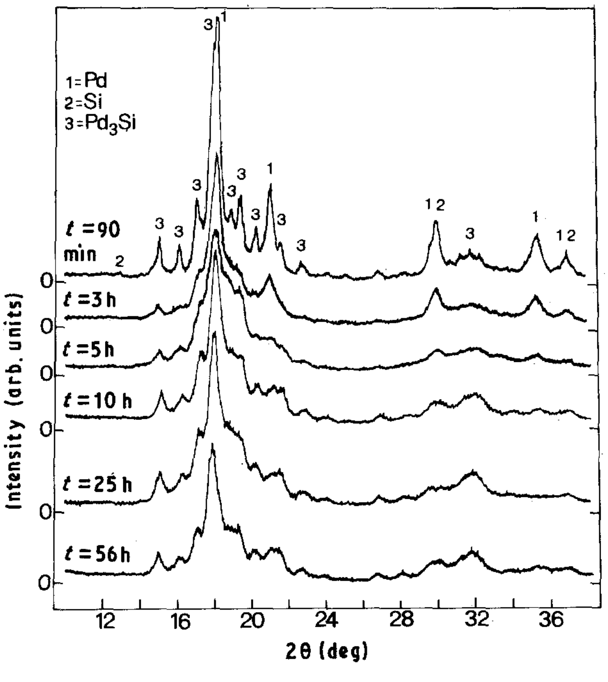

Figure 3 X-ray diffraction patterns of Pd_3Si (F) composition at various milling times.

3.2. Fluorescence data

The fluorescence results, for the same samples monitored via X-ray diffraction, are given in Fig. 6, where

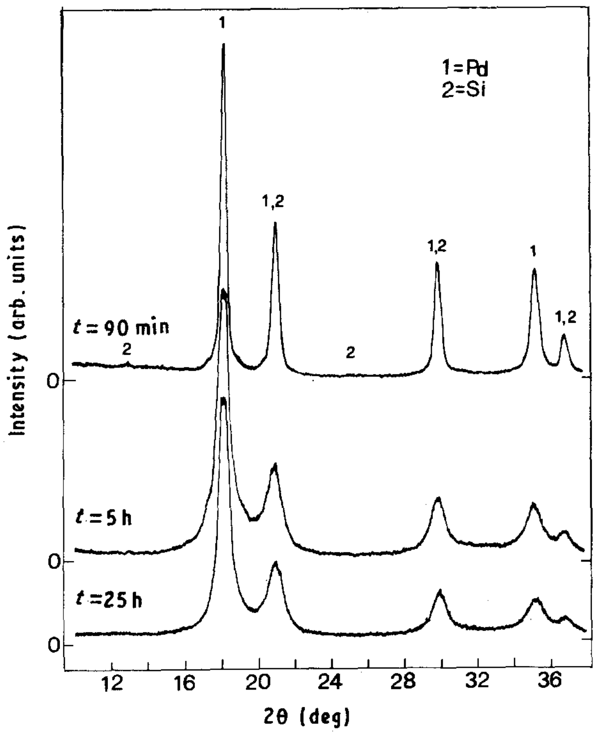

Figure 4 X-ray diffraction patterns of Pd$_5$Si (F) composition at various milling times.

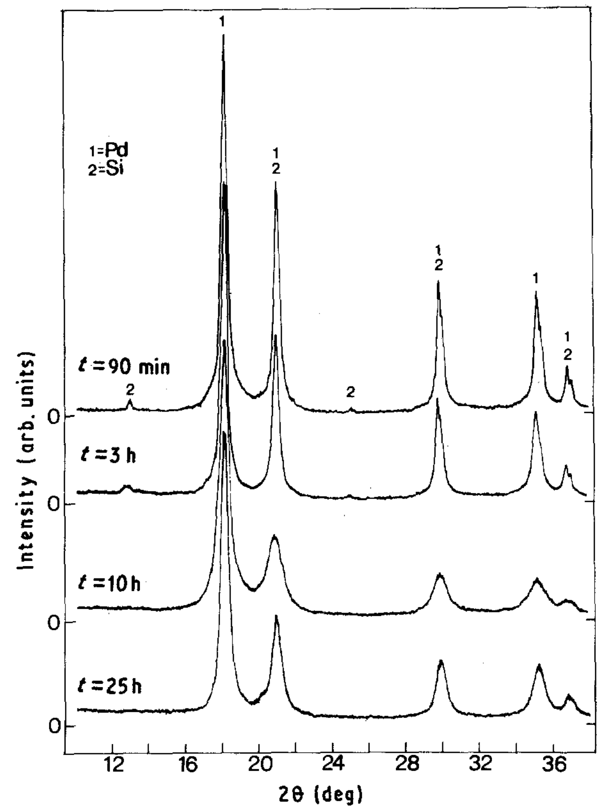

Figure 5 X-ray diffraction patterns of Pd$_4$Si (S) composition at various milling times.

the silicon intensity (%), defined as

$$\text{Si intensity } (\%) = I_{\mathrm{Si}K_\alpha}/(I_{\mathrm{Si}K_\alpha} + I_{\mathrm{Pd}L_\alpha})100 \quad (1)$$

is reported versus the milling time. It can be noticed that after only 1 h milling the signal decreases by about 85%–90% and that at 2 h an asymptotic value is reached for each composition. It must be stressed that the fluorescence signal decay cannot be attributed

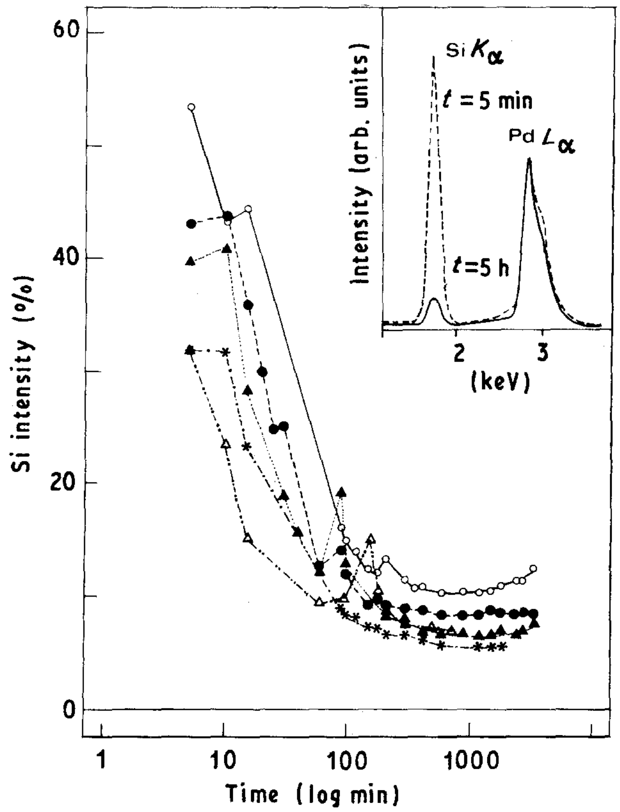

Figure 6 The silicon intensity (%, see text) plotted against the milling time for the compositions examined. For clarity, lines have been drawn connecting the experimental points. The onset shows the emission fluorescence for the Pd$_{2.5}$Si composition after (– – –) 5 min and (——) 5 h milling. The spectra at different times have been normalized with respect to the PdL_α emission at 5 min. (○) Pd$_{2.5}$Si, (●) Pd$_3$Si, (▲) Pd$_4$Si, (∗) Pd$_5$Si, (△) Pd$_4$Si (S).

to a lowering of the silicon content as careful chemical analysis of the final samples demonstrated.

4. Discussion

We have identified several main steps occurring during the MA process and these will be discussed in some detail.

4.1. Intimate mixing

The "intimate mixing" of the constituent particles is well known from the time of classic mechanical alloying when the aim was not, as in recent times, the obtainment of an amorphous or metastable phase but only a fine dispersion of an additive to an already existent powder alloy. The formation of a composite layered structure in the MA process has been well described and documented in both classic [1] and recent investigations [4]. We can now add some information concerning a brittle (Si)–ductile (Pd) binary system from examination of the results of the milling process.

Fig. 7, representative of what typically happens for all compositions, shows broadening of the initial peak lines starting from the very beginning of the process. Both Pd and Si lines are broadened, but while the Pd{3 1 1} integral area remains practically constant from $t = 0$–35 min, the Si{1 1 1} integral peak decreases towards about one-tenth of the initial value. In

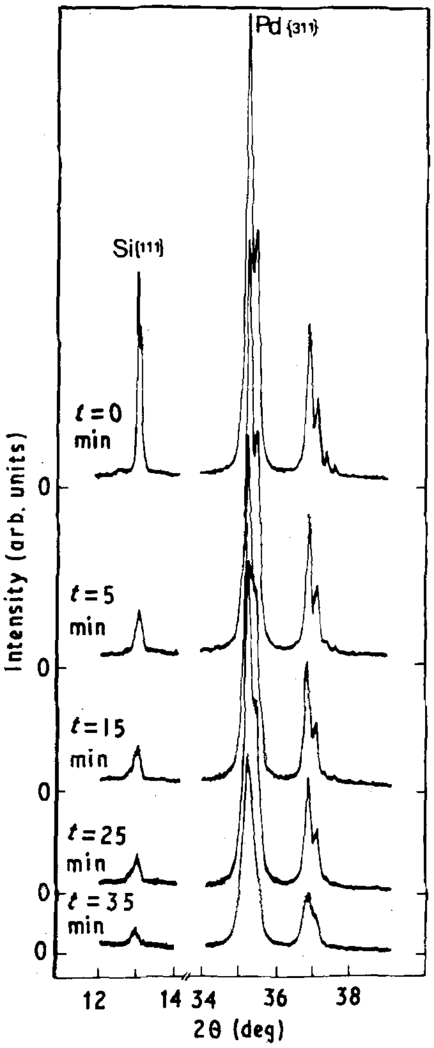

Figure 7 Broadening of the Si{1 1 1} and Pd{3 1 1} peaks, for the Pd_4Si composition, in the early milling stages. The patterns are representative for all the compositions examined.

some patterns the Si{1 1 1} peak seems to vanish even if Pd_3Si does not form (e.g. Fig. 4, Pd_5Si composition). This behaviour can be ascribed to the masking effect of the palladium which governs and reduces the X-ray beam penetration into the sample while the intimate mixing is proceeding.

The absorption coefficients of Si and Pd towards MoK_α radiation are, in fact, markedly different (15.6 and 319.6 cm^{-1}, respectively). Thus the $t_{1/100}$ depth of penetration in pure elements (where $t_{1/100}$ is the depth giving 99% of the diffracted intensity) at 2θ 13° (the Si{1 1 1} peak position) is 167 and 8 μm for silicon and palladium, respectively and 10 μm for a Pd_4Si composition.

Fig. 8 shows a schematic representation of the powder thickness at zero time and after reaching intimate mixing. At zero time the powder is composed of single particles of Si and Pd so that in the volume sampled by the incident beam, the scattered intensity arising from the free silicon particles is appreciable (see Fig. 8a). Once the intimate mixing is realized (see Fig. 8b) it is reasonable to suppose that due to the higher ductility of palladium, the Si particles are homogeneously embedded in the palladium matrix. As a consequence, the depth of penetration is governed by Pd and the integral quantity of silicon present in such a thin layer is insufficient to continue to produce a detectable X-ray diffraction signal.

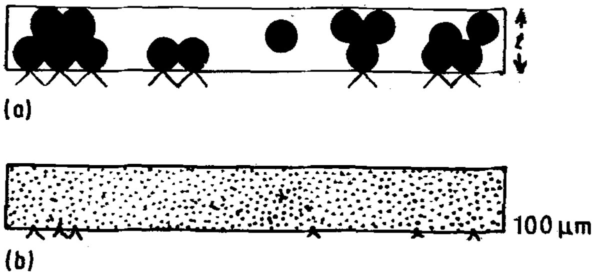

Figure 8 Representation of the powder thickness ($t \simeq 200$ μm) at (a) zero milling time and (b) after reaching intimate mixing. The surface ratio between black (silicon) and white (palladium) areas roughly represents the Pd_4Si composition (for clarity only silicon particles are drawn). Silicon fluorescence emission is evinced at the bottom of (a) and (b) (see text).

The strong decay of the K_α silicon fluorescence emission may be explained on the same basis. The absorption coefficient of Pd towards the K_α silicon emission is more than 20.000 cm^{-1} so that the detected signal only arises from the few particles lying on the very surface of the sample (see Fig. 8b).

Therefore, X-ray and fluorescence data, before Pd_3Si formation, concurrently indicate the same phenomenon of intimate mixing as can be seen in Fig. 9 where the silicon fluorescence emission and the {1 1 1} silicon peak maximum intensity are reported for the first 30 (Pd_3Si) or 35 (Pd_4Si) min milling.

Another point worthy of attention deals with the angular positions of the palladium peaks. As long as they are detectable in any diffraction pattern of any composition (both before and after Pd_3Si formation, see below) they do not show any angular shift. This observation implies that the milling process does not promote a solid solution between Pd and Si and thus does not alter the miscibility gap reported at room temperature in the Pd-rich part of the phase diagram.

4.2. Pd_3Si formation

Once the palladium and silicon components are thoroughly mixed, Pd_3Si formation can occur. After 90 min milling the intermetallic compound is abruptly formed, for all compositions (Figs 1–3) except 5/1 milled in Fritsch and 4/1 milled in Spex (Figs 4, 5).

From the experimental results of Pd_3Si formation, two points arise: the first is related to the composition variation, and the second to the variation of milling conditions for the same composition.

Only the 5/1, composition treated in exactly the same way as all the others, does not form an intermetallic phase. We have also verified that the Pd_5Si composition does not react even when realizing a higher energy transfer by suitably varying the milling conditions (see below). What is noticed, in all cases, is just a broadening of the palladium peak lines while their positions do not shift at all with increasing milling time. In other words, for the 5/1 composition, we have not been able to promote silicon diffusion into the palladium matrix thus allowing Pd_3Si nucleation.

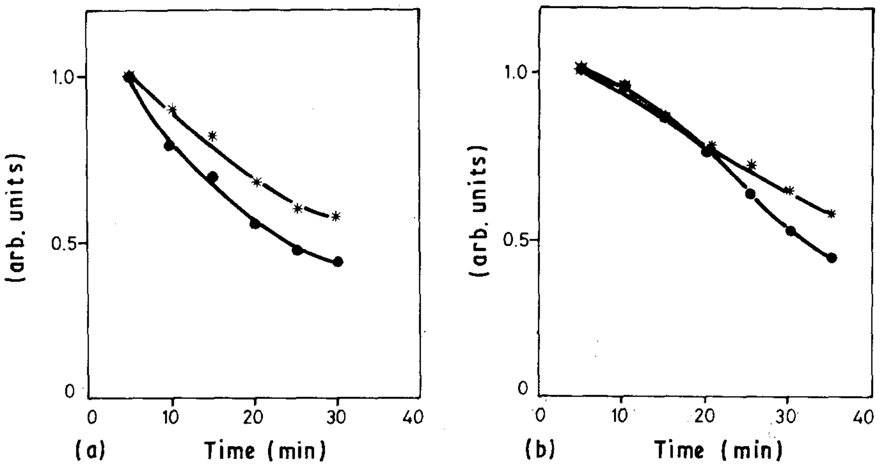

Figure 9 Time dependence of (∗) the silicon fluorescence signal and (●) X-ray Si{1 1 1} peak height. The data, in arbitrary units, have been normalized to unity for both kinds of measurement. Lines have been drawn through the experimental points for a better indication of the trend. (a) Pd_3Si, (b) Pd_4Si.

An emerging link between our experimental findings and the Egami and Waseda correlation [14] should be noted. Analysing literature data on amorphous phase formation by rapid quenching of binary systems, Egami and Waseda found an empirical correlation between the minimum solute concentration, necessary to obtain a "stable" amorphous phase, and the atomic volume mismatch (correlated, in turn, to the atomic sizes). For the Pd–Si system, a minimum of 16.9 at % Si has been predicted. The coincidence of this figure with 16.7 (the atomic composition of Pd_5Si) suggests that the empirical correlation, based on atomic size parameters which are independent of the preparation methods, is somehow valid for the Pd–Si system treated by ball milling. Under the conditions examined, in fact, Pd_3Si has been identified to be the first step, for the 2.5/1, 3/1 and 4/1 compositions (milled in Fritsch), towards an amorphous or a partially amorphous state. If a critical local silicon concentration inside the Pd matrix is never achieved in order to enable Pd_3Si nucleation to occur, the formation of the subsequent amorphous phase will never take place.

The second point, i.e. the effect of varying the milling conditions for the same composition, can be compared for Pd_4Si samples treated in different ways. In the Fritsch apparatus, 90 min milling promotes the Pd_3Si formation (Fig. 1). In the Spex ball mill the Pd_4Si composition never reacts (Fig. 5). In the latter case, a progressive broadening, measured by the half-maximum line width (see Table I), is noticed up to about 5 h milling and then a plateau is reached with no further broadening by prolonged milling. Broadening of the Bragg lines is either due to the reduction of the coherent domains or to the accumulation of strain in the networks. The fact that a plateau region is reached indicates that further milling is really ineffective on both domain size and strain. It is evident that the energy transfer realized in the two milling conditions is different.

We have reported that the energy transferred to the powder during milling is mainly due to the kinetic energy dissipated by the balls hitting the vial walls [15, 16]. The level of energy transfer can therefore be correlated, using analytical equations [15, 16], to the mass of the ball, m_b, and to the velocity of the ball, v_b, launched inside a vial. By suitably varying m_b or v_b different conditions of energy transfer are realized and hence different solid state reactions can be activated. This is precisely what occurred to the 4/1 composition milled under the conditions of Figs 1 and 5.

TABLE I Line booadening of the Pd{3 1 1} peak, expressed in half-maximum line width (B_o), as a function of the milling time for the Pd_4Si composition milled in Spex

t (h)	B_o (2θ deg)
0.1	0.4
2.0	0.4_5
3.0	0.5_5
3.5	0.7
5.0	1.0
10.0	1.0
15.0	0.9
20.0	0.9

To check this point further we chose an intermediate milling condition, and the results of 3 h milling are given in Fig. 10 together with the previous results from Figs 1 and 5. Milling for 3 h under the different conditions (I–III) gives, respectively: (i) broadening of the lines only (Fig. 10a); (ii) amorphous-like phase formation (Fig. 10b) and (iii) intermetallic compound formation (Fig. 10c).

Fig. 11 shows, in a schematic way, the different process promoted by the three different milling conditions. The G_{lb} lines of Fig. 11 represent various states with different defect densities up to a maximum of defects that represent a stationary state over which an amorphous phase is nucleated or the milling results are ineffective, as indicated by the results of Table I, showing no further line broadening after 5 h milling. The energy transfer realized under Condition I is insufficient to overcome the nucleation barrier to form an amorphous phase. Under Condition II the energy transfer is high enough to promote the amorphous phase formation, and under Condition III the intermetallic Pd_3Si compound can be obtained.

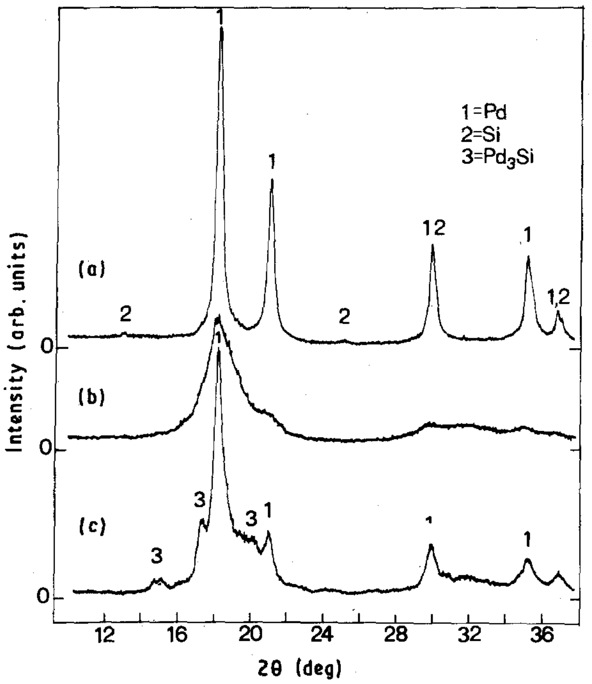

Figure 10 Effect of 3 h milling on the Pd_4Si composition under the following milling conditions: (a) Condition I, SPEX 8000: stainless steel tools with ball diameter = 6 mm; (b) condition II, SPEX 8000: tungsten carbide tools with ball diameter 10 mm; (c) Condition III, Fritsch Pulverisette 5: stainless steel tools with ball diameter = 10 mm and rotation speed of 9/10 of the maximum.

4.3. Stationary state, demixing and thermal treatments

As soon as it is formed, the lines of Pd_3Si begin to broaden, indicating that the possible pathway towards the amorphous phase is of the type

$$\text{Powder mixture} \rightarrow \text{Intermetallic} \rightarrow \text{Amorphous phase} \quad (2)$$

in a manner that has been documented previously [10, 12]. The 4/1, 3/1 and 2.5/1 compositions indicate a probable coexistence of intermetallic and amorphous phase. The metastable situation has been described in a previous paper in terms of a dynamic equilibrium in which the intermetallic fraction transformed to glass by the milling process is compensated by an equal amount of glass experiencing the inverse transformation [12].

Long milling times up to 56 h result in a demixing process for the 4/1 and 2.5/1 compositions (see Figs 1 and 2). The demixing is very clear and undoubtedly goes towards the elemental Pd constituent. The angular positions of the palladium lines after 56 h milling are exactly the same as the starting positions. The fact that silicon lines (or silicon oxide, see below) are not seen can be explained on the same basis as discussed in the previous paragraph and the clear appearance of the Pd lines only, is therefore enough to evince a demixing phenomenon passing through the intermetallic Pd_3Si compound.

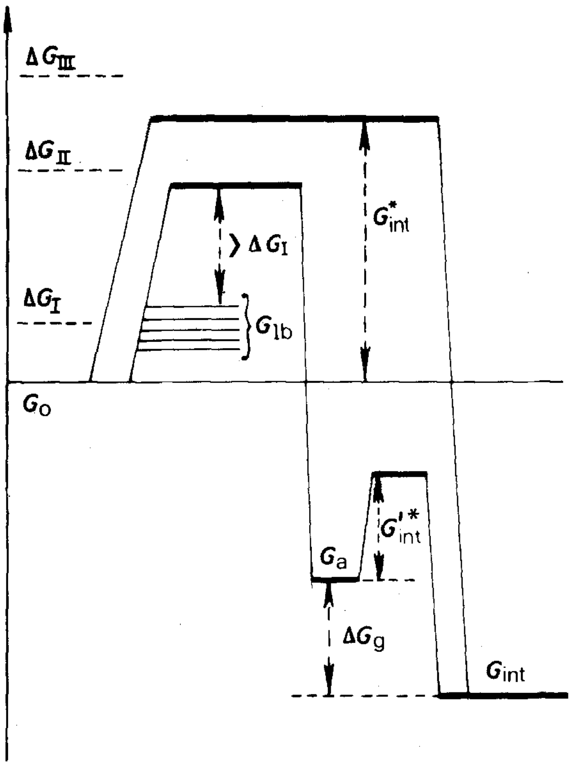

Figure 11 Schematic free energy diagram. G_o, G_{lb}, G_a and G_{int} are the free energies of the initial, the "peak line broadening", the amorphous and the intermetallic states of the Pd_4Si system, respectively. G^*_{int} is the activation energy to form the intermetallic compound. ΔG_I, ΔG_{II} and ΔG_{III} are the energy states during ball impact corresponding to the three milling conditions shown in Fig. 10 (see text). ΔG_g is the grinding energy needed to amorphize the intermetallic compound.

The demixing phenomenon has now been well documented in several cases (see e.g. [16–21]). The common feature is that it always occurs at long milling times. Very likely different phenomena can be encompassed by the word "demixing". In some cases it has been noticed that long milling times, beyond the formation of an amorphous phase, result in apparently new unknown phases [17, 18, 21] and discussion of their nature is an open question. In other cases the phenomenon is probably due to the handling milling procedures introducing contaminations.

In a careful work on Ni–Zr alloys, Mizutane and Lee [19] attributed the recrystallization occurring by milling beyond the amorphous phase formation, to oxygen contamination and/or to iron–chromium impurities (coming from the milling tools). Detection of Zr oxide phases on their Ni–Zr thermally treated samples was considered to support their hypothesis.

In our experience, demixing may or may not occur when milling Fe–Zr alloys under apparently exactly the same conditions [16]. This probably means that contaminations not fully under control may be responsible for the recrystallization.

The present results clearly confirm the Mizutane and Lee observations. Table II shows the level of oxygen contamination for the 56 h milled samples. Oxygen pick-up is noticeable for the 2.5/1 and 4/1 compositions for which the demixing phenomenon has been clearly observed by X-rays. If we compare the heat of formation of SiO_2 ($-880\ \text{kJ mol}^{-1}$ [22]) with that of the intermetallic Pd_3Si ($-37\ \text{kJ mol}^{-1}$ [23]), the demixing process can be explained by the formation of SiO_2 which is more stable than the previously formed Pd_3Si. Supposing that all the oxy-

TABLE II Oxygen content of the 56 h milled samples

Starting composition	Oxygen (wt %)	Real composition	Possible stoichiometry
$Pd_{2.5}Si$	7 ± 1	$Pd_{2.5}SiO_{1.5}$	$(Pd_3Si)_{0.25}Pd_{1.75}(SiO_2)_{0.75}$
Pd_3Si	1.6 ± 0.1	$Pd_3SiO_{0.4}$	$(Pd_3Si)_{0.8}Pd_{0.6}(SiO_2)_{0.2}$
Pd_4Si	3.6 ± 0.2	$Pd_4SiO_{1.1}$	$(Pd_3Si)_{0.45}Pd_{2.65}(SiO_2)_{0.55}$

TABLE III Line broadening of the Pd {3 1 1} peak, expressed in half-maximum line width (B_0), for "demixed" and "undemixed" samples at long milling times. S and F indicate Spex or Fritsch ball mill

	"Demixed" samples		Not "demixed" samples	
	56 h, $Pd_{2.5}Si$ (F)	56 h, Pd_4Si (F)	20 h, Pd_4Si (S)	30 h, Pd_5Si (F)
B_0 (2θ deg)	0.9	0.8	0.9	0.9

gen is present in the form of silicon oxide, the final stoichiometry of the samples is given in the last column of Table II.

The lowest oxygen contamination is detected for the 3/1 composition and this agrees with diffraction data still showing a predominance of Pd_3Si. The fact that at the 3:1 stoichiometry the oxygen pick-up is at a minimum, is probably related to a greater stability of the intermetallic compound formed when starting exactly from its composition.

The broadening of the palladium lines after demixing is nearly the same as that of the long-term milled samples which never reacted (5/1 in Fritsch and 4/1 in Spex). Table III gives the half-maximum line width for both "demixed" and "undemixed" samples. It seems, therefore, that the highest defect density state (e.g. that

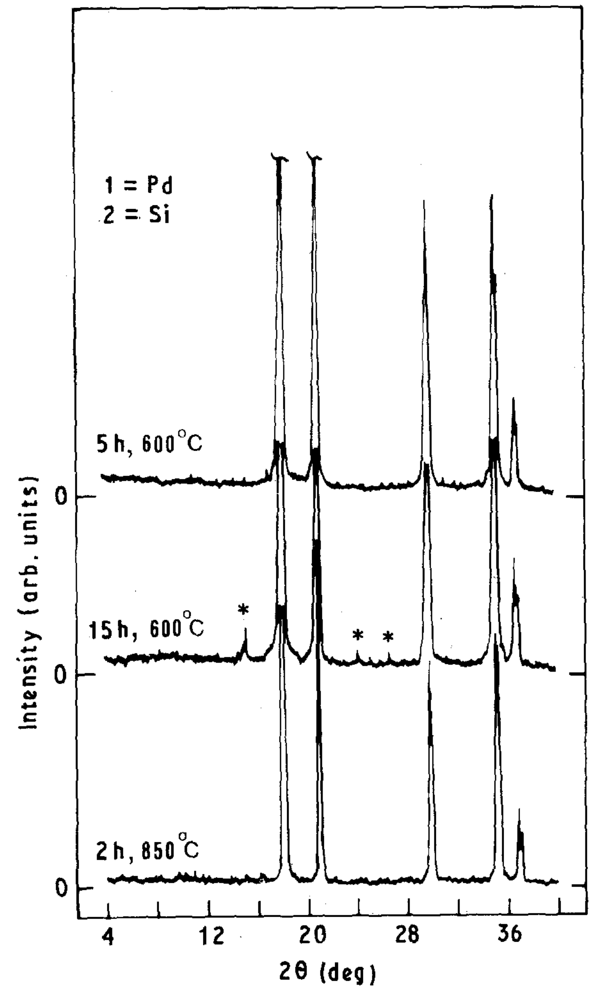

Figure 12 Thermal treatments of the 56 h milled $Pd_{2.5}Si$ sample. The main lines belong to Pd reflections. Asterisks indicate the existence of an unknown metastable phase.

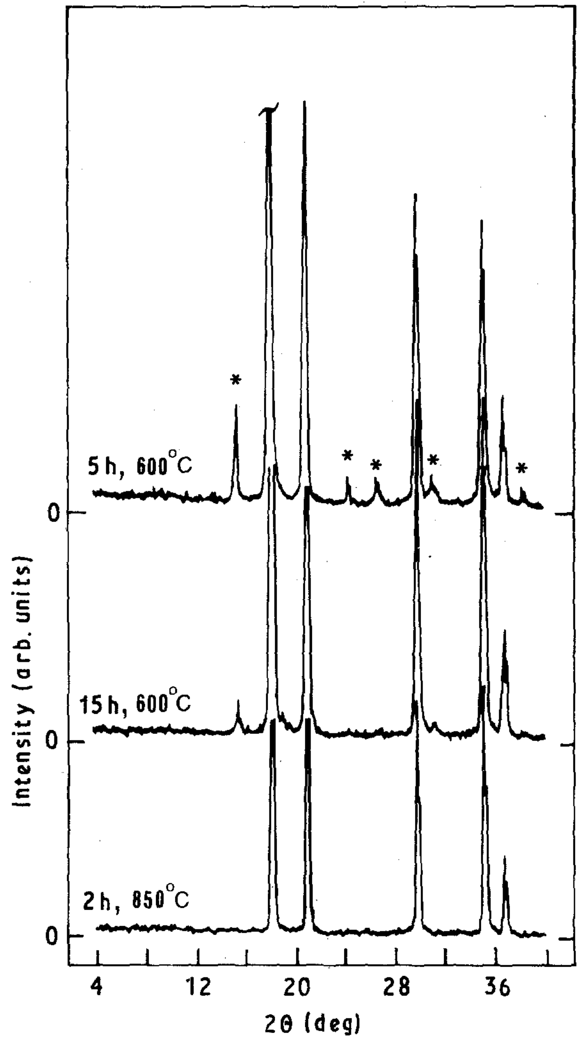

Figure 13 Thermal treatments of the 56 h milled Pd_4Si sample. The main lines belong to Pd reflections. Asterisks indicate the existence of an unknown metastable phase.

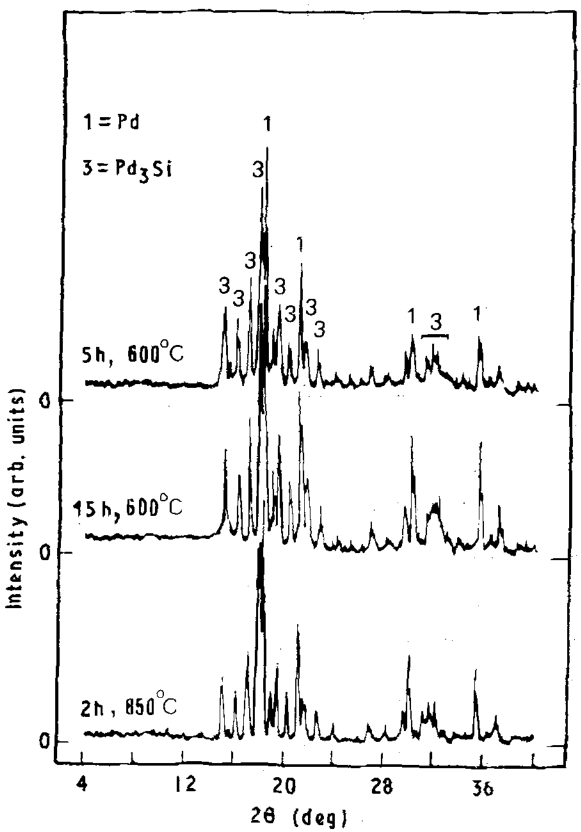

Figure 14 Thermal treatments of the 56 h milled Pd$_3$Si sample.

corresponding to the maximum of the G_{1b} lines in Fig. 11) can be reached by strongly different pathways.

Thermal treatments of the three compositions (2.5/1, 4/1 and 3/1) induce sharpening of the peak line profiles of the 56 h products due to the recovery of lattice defects (Figs 12–14). It is worth noting that the 850 °C treatment, for the 2.5/1 and 4/1 compositions, does not promote any kind of reaction between palladium and silicon, supporting the hypothesis that silicon is present in the highly stabilized form of silicon oxide.

References

1. J. S. BENJAMIN, *Metall. Trans.* **1** (1970) 2943.
2. C. C. KOCH, O. B. CAVIN, C. G. McKAMEY and J. O. SCARBROUGH, *Appl. Phys. Lett.* **43** (1983) 1017.
3. R. B. SCHWARZ, R. R. PETRICH and C. K. SAW, *J. Non-Cryst. Solids* **76** (1985) 281.
4. E. HELLESTERN and L. SCHULTZ, *Appl. Phys. Lett.* **48** (1986), 124.
5. J. R. THOMSON and C. POLITIS, *Europhys. Lett.* **3** (1987) 199.
6. G. ENNAS, M. MAGINI, F. PADELLA, P. SUSINI, G. BOFFITTO and G. LICHERI, *J. Mater. Sci.* **24** (1989) 3055.
7. R. B. SCHWARZ and C. C. KOCH, *Appl. Phys. Lett.* **49** (1986) 146.
8. P. Y. LEE, J. JANG and C. C. KOCH, *J. Less-Common Metals* **140** (1988) 73.
9. B. T. McDERMOTT and C. C KOCH, *Scripta Metall.* **20** (1986) 669.
10. M. S. KIM and C. C. KOCH, *J. Appl. Phys.* **62** (1987) 3450.
11. T. J. TIAINEN and R. B. SCHWARZ, *J. Less-Common Metals* **140** (1988) 99.
12. G. ENNAS, M. MAGINI, F. PADELLA, F. POMPA and M. VITTORI, *J. Non-Cryst. Solids* **110** (1989) 69.
13. N. BURGIO, G. ENNAS, M. MAGINI, F. PADELLA, B. SCHIPPA and P. SUSINI, "Solid State Powder Processing", TMS Conference, Indianapolis, 1–5 October 1989, edited by A. H. Claver and J. J. de Bazbadillo, pp. 343–356.
14. T. EGAMI and Y. WASEDA, *J. Non-Cryst. Solids* **64** (1984) 113.
15. N. BURGIO, A. IASONNA, M. MAGINI and F. PADELLA, *Colloque Phys.* C4-265 (1990).
16. N. BURGIO, A. IASONNA, M. MAGINI, S. MARTELLI and F. PADELLA, *Nuovo Cimento* (1991) in press.
17. G. COCCO, I. SOLETTA, L. BATTEZZATI, M. BARICCO and S. ENZO, *Phil. Mag.* **61** (1990) 473.
18. N. BURGIO, W. GUO, M. MAGINI, S. MARTELLI, F. PADELLA and I. SOLETTA, in "ASM International Conference", Myrtle Beach, 27–29 March 1990.
19. U. MIZUTANI and C. H. LEE, *J. Mater. Sci.* **25** (1990) 399.
20. M. A. MORRIS and D. G. MORRIS, in "Solid State Powder Processing", TMS Conference, Indianapolis, 1–5 October 1989, edited by A. H. Claver and J. J. de Bazbadillo.
21. H. J. FECHT, G. HAN, Z. FU and W. L. JOHNSON, *J Appl. Phys.* **67** (1990) 1744.
22. "Handbook of Chemistry and Physics" (CRS Press, Boca Raton, Florida, 1981).
23. F. R. DE BOER, R. BOOM, W. C. M. MATTENS, A. R. MIEDEMA and A. K. NIESSEN (eds), "Cohesion in Metals" (North Holland, 1988) Ch. III.

Received 16 July
and accepted 19 November 1990